

Loma Linda University

TheScholarsRepository@LLU: Digital Archive of Research, Scholarship & Creative Works

Loma Linda University Electronic Theses, Dissertations & Projects

12-1984

Autoradiography of Photomembrane in HEMIGRAPUS NUDUS

Carol Fulenwider

Follow this and additional works at: <https://scholarsrepository.llu.edu/etd>



Part of the [Physiology Commons](#)

Recommended Citation

Fulenwider, Carol, "Autoradiography of Photomembrane in HEMIGRAPUS NUDUS" (1984). *Loma Linda University Electronic Theses, Dissertations & Projects*. 582.

<https://scholarsrepository.llu.edu/etd/582>

This Thesis is brought to you for free and open access by TheScholarsRepository@LLU: Digital Archive of Research, Scholarship & Creative Works. It has been accepted for inclusion in Loma Linda University Electronic Theses, Dissertations & Projects by an authorized administrator of TheScholarsRepository@LLU: Digital Archive of Research, Scholarship & Creative Works. For more information, please contact scholarsrepository@llu.edu.

Abstract

AUTORADIOGRAPHY OF PHOTOMEMBRANE

TURNOVER IN HEMIGRAPSPUS NUDUS

by Carol Fulenwider

Protein synthesis was studied in the visual cells of Hemigrapsus nudus by light microscope autoradiography. Two hours before sunset, crabs were injected with a single dose of tritiated leucine and sacrificed at time intervals coincident with dynamic retinal changes observed in electron microscope (EM) studies of related Arthropods (Blest, 1978 and Stowe, 1980).

Two separate experiments were performed to examine time periods in the renewal process. Some periods in each experiment were overlapped to develop more accurate decay curves. Experiment I followed time regimes of 0.5, 1.5, 2.5, 3.0, 3.0, 5.0, and 6.0 hours after sunset. Autoradiographs of retinula cells were examined for temporal variations in grain concentration and in spatial distribution patterns. The concentration of leucine in the retinula cells peaked at 1.5 hours, declined until the third hour, and leveled off through hour six. Region II peripheral to the rhabdome showed the highest concentration for all sample times.

In Experiment II, greater resolution of peak times for grain concentration was obtained using sacrifice regimes of 0.0, 0.5, 1.0, 1.5, and 2.5 hours after sunset. Also evaluated were temporal variations in rhabdomeral-cytoplasmic distribution. Other retinula

cells were sampled at 0.5 and 1.0 hours after injection to determine the path of newly-synthesized protein before induction of the dark phase. Finally, similar evaluations of grain count and distribution were performed on autoradiographs of visual cells at sunrise (sample times: 0.0, 1.0, 2.0 hours after sunrise) and after long-term exposure to tritiated leucine (sample times: 1, 2, and 7 days after injection, maintaining normal 12:12 Light:Dark conditions).

Results from Experiment II showed a peak time for grain concentration to be closer to 1.0 hour after sunset rather than the 1.5 hours of Experiment I. Spatially, labeled protein was more concentrated within the cytoplasm until 0.5 hour after sunset, when the higher proportion of grains shifted to the microvilli, the area specialized for light absorption. Long-term samples continued to show the same spatial differentiation while declining in overall count.

LOMA LINDA UNIVERSITY

Graduate School

AUTORADIOGRAPHY OF PHOTOMEMBRANE

IN HEMIGRAPUS NUDUS

by

Carol Fulenwider

A Thesis in Partial Fulfillment
of the Requirements for the Degree
Master of Science in Physiology

December 1984

Each person whose signature appears below certifies that this thesis in his opinion is adequate, in scope and quality, as a thesis for the degree of Master of Science.

Donald D. Rafuse, Chairman
Donald D. Rafuse, Assistant Professor of Physiology

George Maeda
George Maeda, Assistant Professor of Physiology

Robert W. Teel
Robert W. Teel, Associate Professor of Physiology

TABLE OF CONTENTS

OBJECTIVES	1
MATERIALS AND METHODS	9
RESULTS	12
DISCUSSION	19
SUMMARY	27
REFERENCES	28

LIST OF ILLUSTRATIONS AND TABLES

Figure 1.	Horizontal section through Decapod optic lobe	3
Figure 2.	Longitudinal section through optic lobe, and cross-sections of neighboring retinal layers	4
Figure 3.	Graph of Mean Grain Density vs. Time, Experiment I	14
Figure 4.	Histograms of grain densities from regional analysis, Experiment I	15
Figure 5.	Graphs of data from Experiment II	17
Table 1.	Data from Experiment I	13
Table 2.	Data from Experiment II	16

OBJECTIVES

The morphology and cycling of photomembrane in some rhabdomeric Arthropods is analogous in several ways to photomembrane in vertebrates. The rod outer segment (ROS) of vertebrate eyes contains stacks of free-floating discs which are continuously synthesized from the innersegment and slowly migrate proximally until ingested by the basement epithelium. In contrast, photoreceptor cells of most Crustaceans and some Arachnids contain opposing layers of ordered microvilli which are continuous with their cells of origin, the retinula cells. In addition, photoregeneration in some rhabdomeric species is diurnal and temporally separated into breakdown and renewal phases. Such Arthropod visual systems are an excellent source for study of individual phases of cycling, of underlying cellular phenomena, and of regulating factors.

The object of this research is to study membrane renewal in the visual cells of Hemigrapsus nudus, a genus which demonstrates one of the most rapid and radical phase-related changes in cytoarchitecture as yet studied in rhabdomeric invertebrates (Stowe, 1980; Nassel and Waterman, 1979). Using the technique of autoradiography, the path of newly-labeled retinula cell protein is traced and the grain distribution analyzed to determine temporal and spatial patterns of protein distribution. Particular emphasis is placed on evaluation of protein distribution in retinula cells with respect to the dark phase, the light phase, and long-term samples.

To date, research using autoradiography to examine light and dark-related changes in the visual cells of compound eyes have not considered circadian effects on membrane cycling. This research

project, therefore, offers new insight into the evolution of newly-synthesized protein and raises questions concerning procedures and data reported in previous experiments. Before presenting materials and methods, a brief description of crab ommatidia and cycling of photomembrane will be given.

General Description of Decapod Retina

The visual unit of Decapods is the ommatidia composed of an outer cornea, crystalline cone, and retinula cells with axons extending through the basement membrane into the laminal layers. Between the basement membrane and the lamina ganglionaris is a cavity or hemocoel through which hemolymph flows (Figure 1).

The retinula cells in groups of seven (R1-R7) are radially ordered around a central light-gathering rhabdom, an arrangement that has been compared to sections of an orange (Eguchi et al., 1973). The rhabdom is composed of an elaborate system of alternating layers of tightly-packed microvilli or rhabdomeres formed by each retinula cell contributing microvilli from one side of the cell and extending half-way across the diameter of the rhabdom. Facing one direction only, rhabdomeres are aligned at right angles to neighboring microvilli and at right angles to incident light (Figure 2). It is believed that retinula cells concentrate photopigment within the plasma membrane of these rhabdomeres to designate the rhabdom as the locus of the primary photochemical event in vision. In Hemigrapsus, an eighth retinula cell, R-8, contributes microvilli distally and is associated with detection of polarized light. Though variable

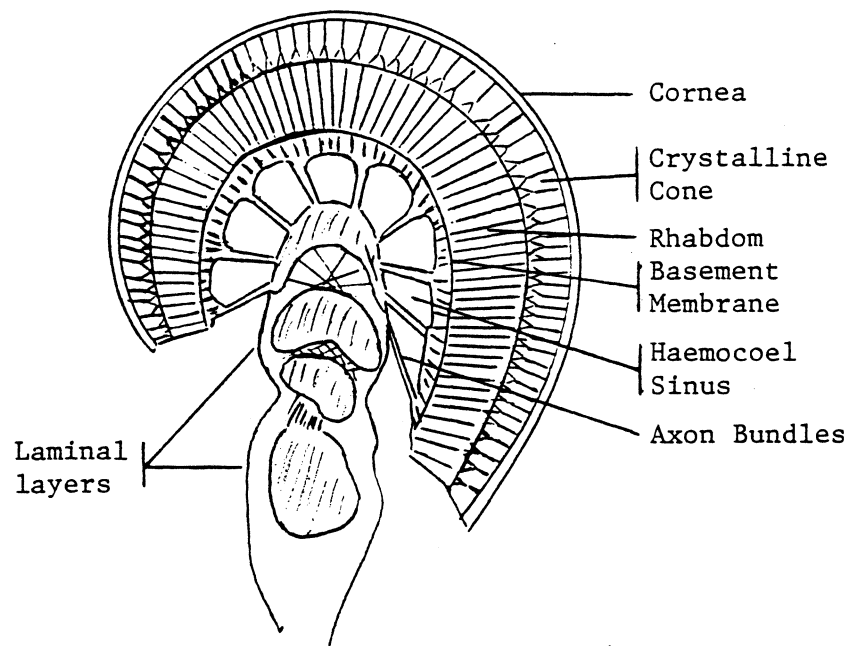


Figure 1. Horizontal section through optic lobe of a typical Decapod, showing ommatidia and laminal layers.

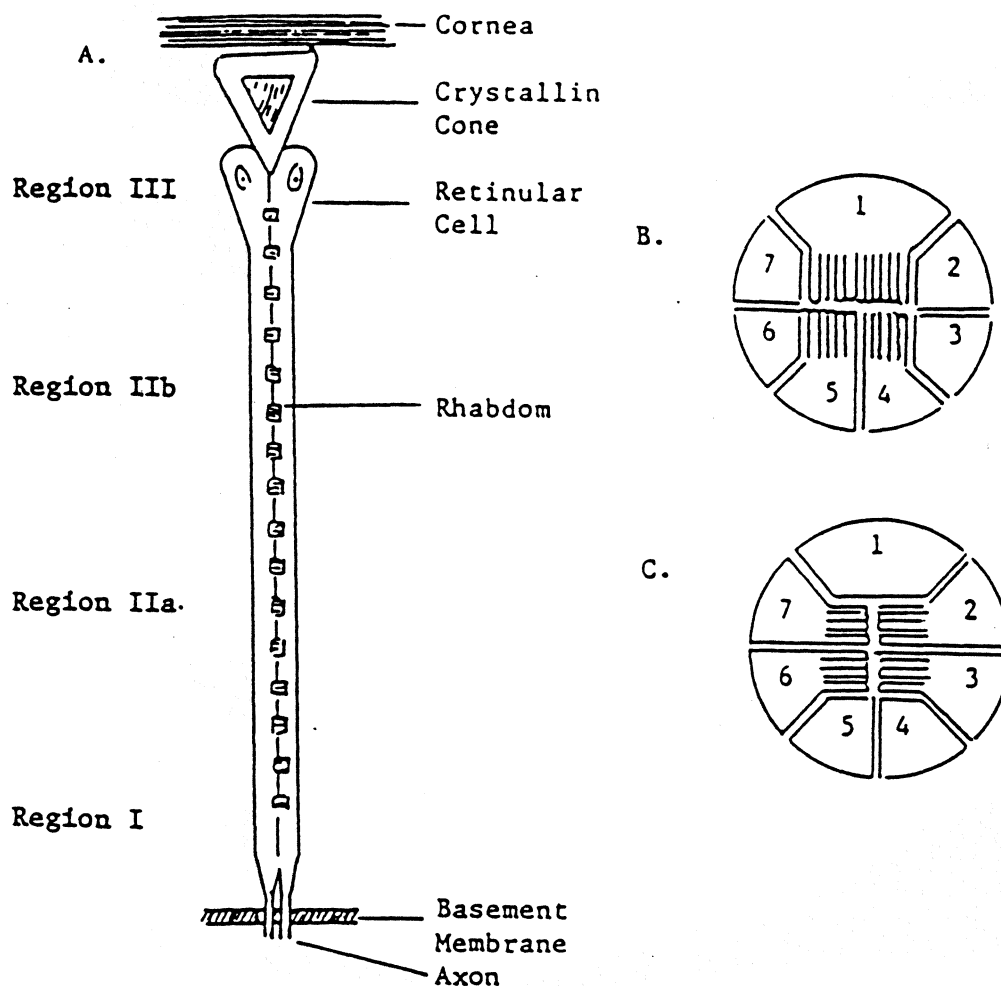


Figure 2. Ommatidial structure in typical compound eye of a Decapod.
 A. Longitudinal section through the optic axis.
 B. Cross-section through retinula showing the make-up of one rhabdom layer: three rhabdomeres running in parallel directions from the retinula cells 1, 4, and 5.
 C. Cross-section of an adjacent rhabdom with rhabdomeres 90° to those of adjacent layers and derived from retinula cells 2, 3, 6, and 7.

in size and geometry among Crustacea, the membrane system in rhabdomes is analogous to outer segments of vertebrate rods and cones.

The major cytoplasmic components are mitochondria, pigment granules, microtubules, and abundant rough and smooth endoplasmic reticulum. A vacuole system surrounding the rhabdoms, the palisades (Horridge and Barnard, 1965).

Cycling of Photomembrane

The first reports showing light-related cytoplasmic changes in photoreceptor cells were made by White (1967, 1968) in the larval mosquito Aedes and by Eguchi and Waterman (1966) in the spider crab Libinia. It is worth noting that shedding and renewal of transductive membrane in vertebrates was being discovered at about the same time (Young, 1967 & 1968; Droz, 1967). Other Arthropods have since been studied regarding the influence of the light and dark phase on retinula cells of compound eyes, e.g., brine shrimp Artemia (Eguchi and Waterman, 1966), Leptograpsus (Stowe, 1980), the net-casting spider Dinopsis (Blest, 1978, 1979, 1980), crayfish Procambarus (Eguchi and Waterman, 1966 & 1976; Hafner and Bok, 1977; Chamberlain and Barlow, 1979), shrimp Palaemonetes (Itaya, 1976), Limulus (Burnel et al., 1970), honeybee (Pepe and Bauman, 1972), muscoid fly (Williams, 1982), and mosquito (Brammer et al., 1978).

Some Arthropods provide excellent material for study of photomembrane cycling (e.g., Grapsus, Libinia, Leptograpsus, Dinopsis, Aedes) because degradation and synthesis of microvillar membrane occurs separately at dawn and dusk respectively. Other Arthropods may be

less amenable to analysis because the mass effects at dawn (Chamberlain and Barlow, 1979, for Limulus), or the synthesis and breakdown are concurrent (White and Lord, 1979, for mosquito). Particularly advantageous to study are Grapsus and Dinopsis, not only for the clear separation of phases in photomembrane cycling but also for their dramatic alteration of rhabdomes between light and dark adapted states. In Grapsus, the difference in rhabdom area between the two states is twenty-fold; in Leptograpsus, whole rhabdomeres are postulated to break down by dusk and to be replaced by freshly-synthesized membrane.

Photomembrane cycling actually represents two independent cycles in retinula cells, one occurring in a burst at dusk and responsible for synthesizing transductive membrane, the other occurring some twelve hours later at natural dawn, internalizing and degrading the membrane. Control of the two phases of the daily cycle has barely been explored, though many Arthropods depend in part on states of illumination to maintain the two cycles (Horridge and Blest, 1980) and turnover is indirectly under the influence of a circadian rhythm.

The phases of photomembrane cycling have generally been defined in terms of the behavior of cytoskeletal components. Induced by light, degradation in most species is an orderly process of membrane breakdown at the base of the microvilli by pinocytosis or by extracellular shedding. Resulting coated vesicles are incorporated into multivesicular bodies and are either lysed or further degraded into residual bodies (Eguchi and Waterman, 1976; Blest, Kao, and

Powell, 1979; Blest, 1978). Also observed during degradation are primary lysosomes and the appearance of acid phosphates (Blest, Price, and Maples, 1979; Blest, Stowe, and Price, 1980). According to Blest (1980), it is doubtful that any components are shunted back unaltered to the rhabdom after being shed. In contrast, synaptic membrane appears to be largely recycled through local systems without being degraded. Since recycling of synaptic vesicles is so rapid and on so large a scale, degradation and resynthesis of their components would be uneconomical.

Less is known about membrane synthesis than breakdown and removal. One characteristic of the cycling rhabdomere of Grapsus is a change in rhabdome volume. In this species, the dark-adapted rhabdome expands to 20X its light-adapted state. Other features of the synthetic state noted by Blest (1980) are the lack of mass production of coated vesicles and multivesicular bodies. More generally, Itaya (1976) hypothesized a model based on EM observations of photomembrane cycling in the shrimp Palaemonetes. He proposed a route for membrane aggregates or "concentric ellipsoids" that starts at the smooth endoplasmic reticulum (ER), moves to the base of microvilli, and organizes into the highly-ordered microvillus pattern of a fully-differentiated rhabdomere. Ongoing work by Stowe on Leptograpsus substantiates and further develops Itaya's model. She showed that microvilli assembly is a process of membrane flow excluding the use of Golgi apparatus and therefore different from synthesis of RDS disc or formation of intestinal brush border cells. According to her work, new membrane differentiates from rough ER as tubules of smooth

ER, is transformed into concentric ellipsoids ("doublet ER") which are transported through the palisades to the rhabdome region. Once in the rhabdom, new microvilli are assembled in situ from sheets of doublet ER which are converted to tubules oriented in the proper direction. The ER becomes progressively narrower, partly by longitudinal division, until the final diameter of microvilli is achieved.

MATERIALS AND METHODS

Crabs (Hemigrapsus nudus) were collected at San Simeon, CA, and maintained at $12 \pm 2^{\circ}\text{C}$ in recirculating sea-water tanks. Fluorescent lights maintained on a 12:12 Light:Dark (LD) cycle provided illumination.

Eight crabs in Experiment I and 15 crabs in Experiment II were injected with 0.2 ml Leucine, L-[4,5- $^3\text{H}(\text{N})$], specific activity 50 Ci/mmol, (New England Nuclear, Boston, Mass.), diluted 1:10 with crab Ringers solution. Each animal was injected 2 hours before sunset to coordinate with initial changes observed through EM studies in the resynthesis process in a similar crab, Leptograpsus (Stowe, 1980). Animals were then sacrificed at the following time regimes: Experiment I: 0.5, 1.5, 2.5, 3.0, 4.0, 5.0, and 6.0 hours after sunset. Experiment II: 0.5 and 1.0 hours after injection; 0.0, 0.5, 1.0, 1.5, 2.0, and 2.5 hours after sunset; 0.0, 1.0, 2.0 hours after sunrise; 1, 2, and 7 days after injection.

Crabs used for control were not injected with leucine but were prepared for histological examination with the experimental crabs as follows. Eyestalks were injected with a pre-fix of 6% gluteraldehyde and 4% formaldehyde in 5ml pipes buffer plus 1.38 grams sucrose, and immediately dissected with the aid of a dissecting microscope. Eyes were fixed overnight in Bovin's fluid (1:22% Picric acid and 40% formaldehyde in glacial acetic acid). The next day, eyes were dehydrated through a 50-75-95-100% alcohol series into xylene, placed in parafin in a 75°C oven and embedded in a peel-a-way mold. Blocks were sectioned at $10\text{ }\mu\text{m}$ and allowed to dry overnight on a slide warmer at 50°C .

In a darkroom, slides were dipped into Kodak NBT-2 Nuclear Track

Emulsion, diluted 1:1 with deionized water and warmed in a 50°C waterbath. Slides were then air dried on a rack and placed in a dark container which was sealed on all sides with black electrical tape. After two weeks of exposure, slides were developed in Kodak D-19 Developer for five minutes and fixed for eight minutes. After being washed in xylene, sections were stained for background with eosin and coverslips added. Autoradiographs were examined under a Zeiss microscope and a camera lucida was used to project grid patterns for a differential counting.

A separate series of crab's eyes, also injected with H^3 -Leucine, were prepared by EM techniques for thinner and clearer tissue sections; however, these sections yielded inconclusive results. The slick epon surface did not allow adhesion of a smooth monolayer of emulsion.

Quantitative Analysis of Autoradiographs

Sections were analyzed under a Zeiss microscope at 80X magnification by projecting ruled drawings onto ommatidia with a camera lucida and counting the number of silver grains overlaying each area. To determine the proximal-distal differentiation of grain distribution for Experiment I, the projections were longitudinally quartered. The area proximal to the basement membrane was designated as Region I, the microvillar area as Regions IIa & IIb, and the distal nuclear area as Region III (Fig. 2A). Counts were made for each region in 30 ommatidia per sample and the grain density (grains/ μm^2) found in order to calculate the mean density/region and the standard error of the mean (SEM). The mean count for ommatidia per sample was derived by totaling the count for the four regions, calculating the number

of grains/ μm^2 /ommatidium, then finding the mean. All grain density values were corrected for background activity and for activity due to the presence of free amino acids bound by fixative, using the 4% figure of Peters and Ashley (42).

Sections from Experiment II were analyzed for grain patterns within different areas of the ommatidium, the rhabdom, and the cytoplasm. Camera lucida projections were used only to determine ommatidium length for calculating density, as diameters for ommatidia and rhabdom remained constant, and separation of grains for counts within the cytoplasm and rhabdom could be done visually. As with Experiment I, 30 ommatidia were counted for each sample time, corrected for background activity, calculated for grain count/ μm^2 , for rhabdomeral and cytoplasmic areas, then calculated for mean grain count/ μm^2 and SEM. Mean counts/ommatidia for each sample were derived by taking the sum of the two areas, finding the number of grains/ μm^2 /ommatidium, and deriving the mean. Proportional values (% count rhabdome and % count cytoplasm, Table 2) were derived by dividing the mean area density (grains/ μm^2 /rhabdom or /cytoplasm) by the total mean density (grains/ μm^2 /ommatidium). The absolute value of grain densities varied considerably between the two experiments, but the relative intensities were constant.

The presence of cytoplasmic pigment granules did not complicate grain counting, a common problem in EM autoradiography. Confusion between label and pigment granules was eliminated since the plane of focus for silver grains was slightly above that for pigment granules.

RESULTS

Thirty minutes after injection with tritiated leucine, the radioactive leucine was found within cytoplasmic and microvillar areas of retinula cells (Table 2 and Figure 5). Because of a higher proportion of counts within the cytoplasm (approximately 75%), it is assumed that newly synthesised protein first appeared in this area. These findings parallel the path of protein in retinal rods where the inner segment is the site of protein synthesis (Besharse et al., 1977; Droz, 1967). One hour after injection, there was an increase in number of grains within the ommatidia and a slightly higher grain count concentrated in the rhabdom.

Thirty minutes after sunset, the pattern of silver grain distribution changed; the silver grains were concentrated in the rhabdom and continued to predominate in that area of the ommatidia. The occurrence of this shift early after the onset of dark correlates with EM findings of rapid synthesis at dusk in Leptograpsus. Examination of decay curves for temporal variations in total grain count (Tables 1 and 2, Figures 3 and 5) show a peak close to one hour after sunset. The occurrence of maximum grain concentration with a shift in grain pattern so early after dusk further supports the rapidity of the reassembly process and the link between induction of membrane turnover with change in the light phase (Basinger et al., 1976; Blest, 1978; Burnel et al., 1970; Besharse et al., 1977; Chamberlain and Barlow, 1979; LaVail, 1976; Young, 1967; Nassel and Waterman, 1979 and Stowe, 1981).

The four regions within the retinal cells examined in Experiment I

	Time After Sunset (Hr)						
	0.5	1.5	2.5	3.0	4.0	5.0	6.0
Ommatidial							
Mean Density ($\text{Gr}/\mu\text{m}^2$)	19.3	24.7	18.8	15.7	11.7	10.2	12.3
SEM	0.8	0.9	0.7	0.7	0.5	0.5	0.6
<hr/>							
Region I ($\text{Gr}/\mu\text{m}^2$)	13.7	21.0	14.2	15.6	9.2	9.9	10.8
SEM	0.7	0.8	0.7	0.7	0.6	0.6	0.7
<hr/>							
Region IIa ($\text{Gr}/\mu\text{m}^2$)	21.7	22.7	21.3	15.7	12.7	10.1	12.9
SEM	0.9	0.8	0.8	0.7	0.6	0.5	0.6
<hr/>							
Region IIb ($\text{Gr}/\mu\text{m}^2$)	21.0	31.9	21.6	15.8	12.3	11.0	13.8
SEM	0.9	1.0	0.8	0.7	0.5	0.6	0.6
<hr/>							
Region III ($\text{Gr}/\mu\text{m}^2$)	20.6	23.2	16.1	15.6	11.8	10.8	11.9
SEM							
<hr/>							

Table 1. Data from Experiment I showing mean density of whole ommatidia \pm SEM for each sample time and regional distribution in $\text{Gr}/\mu\text{m}^2 \pm$ SEM. Values for ommatidial mean density were derived by totaling the number of grains in each of 30 ommatidia in one crab, calculating the density/ommatidium, and finding the mean for the 30 ommatidia. In the same manner, regional density values were derived for each designated area.

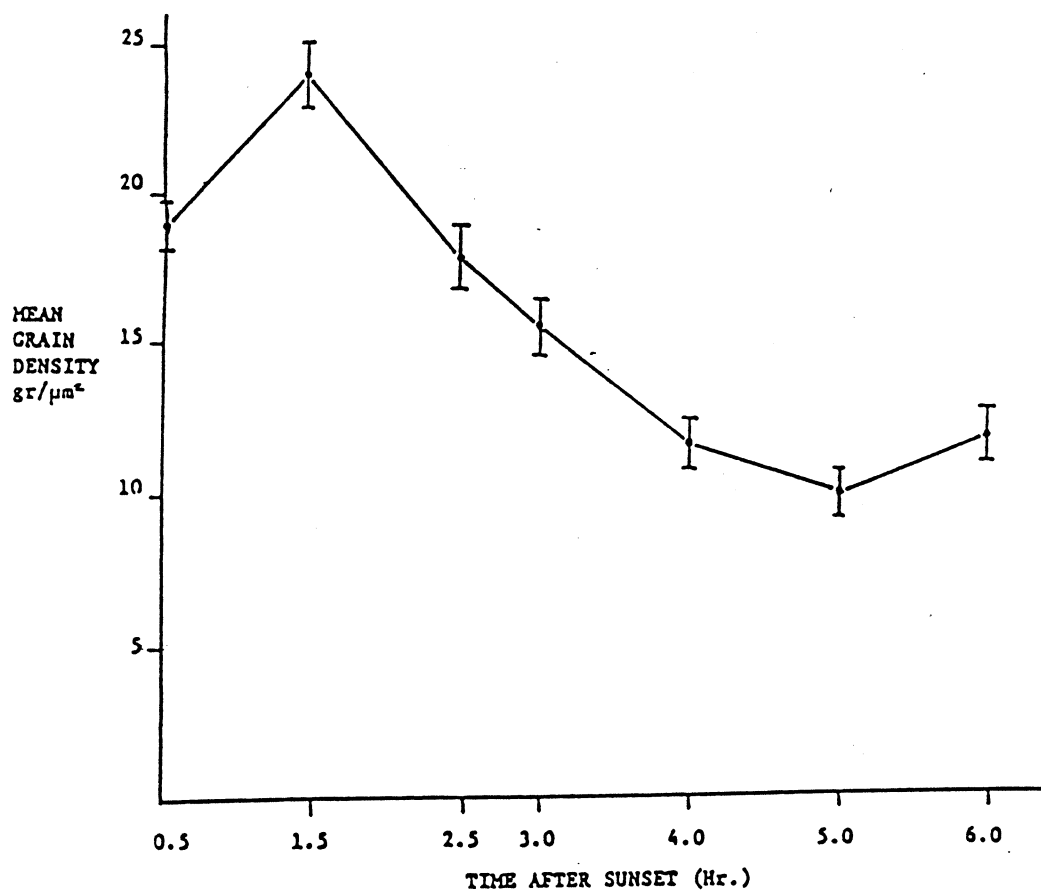


Figure 3. Graph of mean grain density \pm SEM for whole ommatidium for each sample time, Experiment I. Each point on the graph represents the mean of grain counts from 30 ommatidia in one crab.

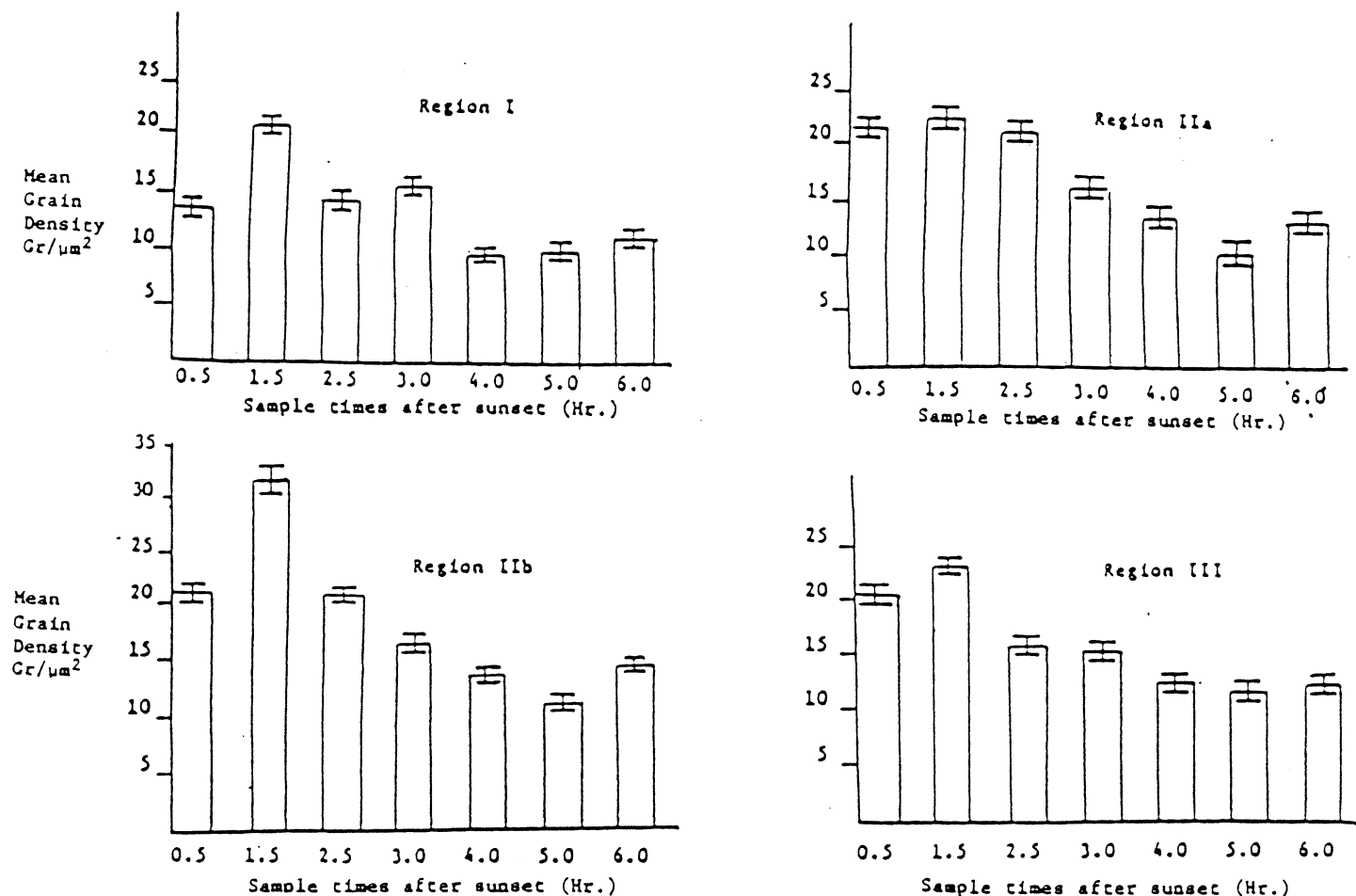


Figure 4. Histograms of grain counts from Regions I, IIa, IIb, and III. Regions represent proximal-distal quaters of whole ommatidium, Region I the most proximal and Region III most distal. Each bar for a designated region reflects the mean density for 30 ommatidia in one crab.

<u>Incorporation Time</u>	<u>Ommatidial Mean Density Gr/μm^2 + SEM</u>	<u>% Count Rhabdom % + SEM</u>	<u>% Count Cytoplasm % + SEM</u>
After Injection (Hr)			
0.5	5.8 \pm 0.3	26 \pm 1.1	74 \pm 3.3
1.0	9.5 \pm 0.5	34 \pm 1.6	66 \pm 3.1
After Sunset (Hr)			
0.0	12.9 \pm 0.6	43 \pm 1.8	57 \pm 2.6
0.5	14.2 \pm 0.7	52 \pm 2.6	48 \pm 2.4
1.0	16.7 \pm 0.7	59 \pm 2.6	41 \pm 1.8
1.5	15.7 \pm 0.6	67 \pm 2.7	33 \pm 1.3
2.0	14.1 \pm 0.6	63 \pm 2.7	37 \pm 1.5
2.5	11.9 \pm 0.6	67 \pm 3.3	33 \pm 1.3
After Sunrise (Hr)			
0.0	13.3 \pm 0.5	65 \pm 2.9	35 \pm 1.5
1.0	12.7 \pm 0.6	58 \pm 2.7	42 \pm 2.0
2.0	12.9 \pm 0.5	54 \pm 2.2	46 \pm 1.8
After Injection (Days)			
1	7.3 \pm 0.3	53 \pm 2.4	47 \pm 2.2
2	5.2 \pm 0.3	58 \pm 3.3	42 \pm 2.4
7	0.9 \pm 0.3	61 \pm 2.7	39 \pm 1.8

Table 2. Data from Experiment II. Mean ommatidial counts for each time period were derived by totaling the grain count in each of 30 ommatidia, calculating the density/ommatidia, then finding the mean for the 30 samples. For proportional counts, the mean density/region for each time period was derived as above, then divided by the appropriate mean density/ommatidia.

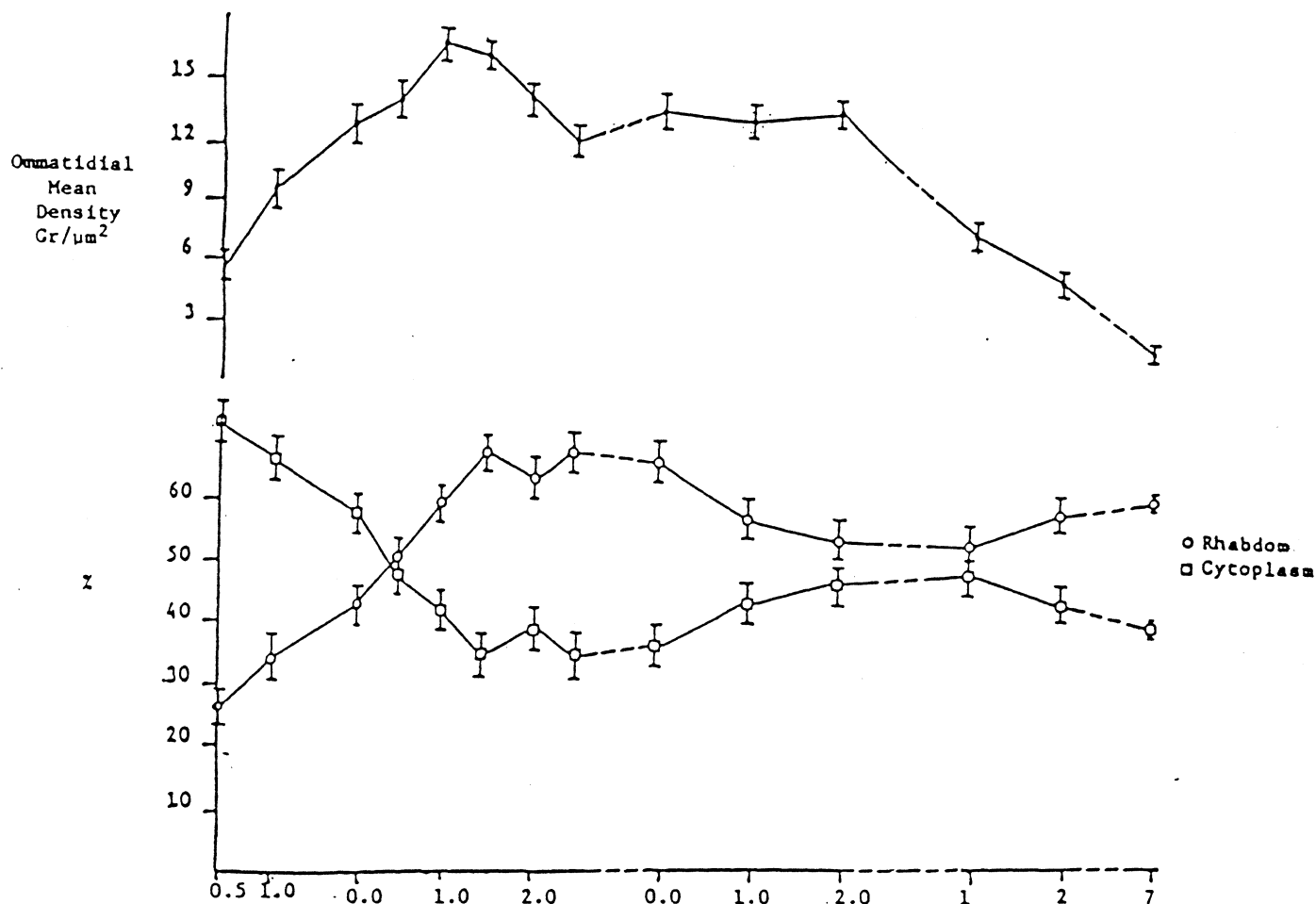


Figure 5. Graphs of data from Experiment II. Upper curve shows mean ommatidial density \pm SEM. Each point on the curve represents the mean density of 30 ommatidia in one crab. Lower curve shows the proportion of ommatidial counts in the rhabdom \circ and the cytoplasm \square .

also exhibited temporal and spatial patterns of labeling (Figure 4). Generally, temporal changes in grain concentration were the same for all four regions, showing a maximum count at 1.5 hours, with a decline and leveling off in the later hours. Spatially, the microvillar region, Region II, contained a higher mean grain density than the nuclear or axonal regions, with Region IIb slightly higher than Region IIa. The gradient may reflect areas of greater protein synthesis or areas with different cellular functions.

At sunrise, the decay curve for total grain count showed little change while the spatial distribution became more evenly spread between microvillar and cytoplasmic areas. By 24 hours after injection, both areas displayed a proportional loss in total count. Two days after exposure to leucine, total grain count continued to diminish until the seventh day, when the number of silver grains was only slightly higher than background count. The rhabdom, however, showed a slight increase in percent of labeled protein.

DISCUSSION

The research described above examines the turnover of photomembrane in the crab Hemigrapsus nudus. Particular attention is given to the assembly of new membrane in the renewal phase which begins rapidly at dusk, with some focus on the degradation phase at dawn and on long-term samples. In the following discussion and interpretation of data, it is assumed that silver grains indicate sites at which radioactive leucine has been incorporated into the proteins of the visual receptor cells (Droz and Warshawsky, 1963).

Renewal Phase

Results from Experiment II show that after a single dose of tritiated leucine, radioactivity appears first in the cytoplasm of visual cells and then in the rhabdomeric microvilli. Since ribosomes have been shown to be present only in the peripheral cytoplasm of visual cells, it may be assumed that protein synthesis occurs in this area of the cell and that radioactivity in the rhabdom arises through a migration of protein from the cytoplasm rather than from slower synthesis of protein in the rhabdom. A second feature of leucine uptake as shown in Figure 5 is the movement of labeled leucine from the cytoplasm to the rhabdom. This suggests a concentration of de novo protein by the visual cells into the microvilli.

This pattern of protein synthesis and transport resembles that described in vertebrate visual cells (rods and cones). Autoradiography experiments with frogs (Hall et al., 1969) and rats and mice (Droz, 1967) show that injected amino acids are rapidly incorporated into newly synthesized protein in the retinal inner segment, predominantly on the

ribosomes. These radioactive proteins are assembled into basal membranous discs of the outer segment following a period of migration (30-60 min.) within the inner segment.

An important point in the interpretation of data is revealed by Perrelet (1972) using autoradiography to study visual cells in the honeybee drone, an insect with ommatidia structurally and functionally similar to the crab. He showed that radioactivity, though decaying, persists in the hemolymph beyond two days, a finding which means that data presented in this paper did not evolve from a true pulse experiment. It is probable that labeled protein was continuously available to visual cells through the hemolymph and it is therefore not possible to visualize a single front of newly synthesized proteins moving from one compartment to another.

By examining longitudinal rather than horizontal distribution of grains in Experiment I, a different type of grain pattern during the renewal phase was demonstrated. The data showed a differential distribution of radioactivity along a proximal-distal axis (Regions I-III) with higher levels of protein synthesis in the central portion of the ommatidia (Region II). Although the rhabdom area was included in regional counts, it is unlikely that this area contributed to the unequal spread of grains, as studied with EM autoradiography in crayfish (Hafner and Bok, 1977) show an uneven count along the length of microvilli through 12 hours after injection (Note: this research did not examine differential counting in the cytoplasm). It is therefore likely that the cytoplasm along was responsible for the longitudinal grain pattern and that the region of cytoplasm peripheral to microvilli

containing the highest proportion of counts represents the area of greatest protein synthesis. EM studies localizing abundant endoplasmic reticulum adjacent to the edges of the rhabdom agree with the above data.

The picture presented thus far of the cytoplasm as the site of protein synthesis and areas peripheral to the rhabdom as the most active, supports a model proposed by Itaya in his study of microvillar membrane formation in the shrimp Palaemonetes and further developed by Stowe in her studies on Leptograpsus. The model proposes that new membrane is synthesized in the cytoplasm on rough endoplasmic reticulum (ER) and forms tubules of smooth ER that roll into "doublet ER" which move through the palisades into the rhabdomeral region where microvilli assemble from the doublet form. Unlike ROS discs, photomembrane formation in ommatidia excludes the use of Golgi apparatus and represents an example of membrane flow from the site of synthesis to the site of incorporation in the microvilli. Membrane protein is most likely inserted into the preformed membrane.

Other studies with vertebrate ROS (Hall et al., 1969) and mosquitoes (Stein et al., 1979) add further information by identifying the majority of new protein as opsin, which, when conjugated with retinene, forms rhodopsin. Data from Experiment II showing preferential accumulation of label in the rhabdom not only point to the path of migration of newly-synthesized protein, but also endorse the suspected functional nature of the rhabdom, that of light absorption. The picture now becomes one of synthesis of opsin as the major component of new membrane and its concentration in the rhabdom.

Other characteristics of the renewal phase can be seen upon examination of the curve for temporal changes in total grain count (Figure 3 and Figure 5, upper curve). An early peak, approximately one hour after sunset, reflects a rapid rate of renewal, a finding supported in EM studies by Nassel and Waterman on Grapsus (1979). This rock crab, along with Dinopsis, represents an extreme in photomembrane turnover as light and dark-adapted eyes differ nearly 20-fold in photoreceptor membrane area. Reports from Stowe on Leptograpsus imply that nearly complete reassembly of rhabdomeres is accomplished within 30 minutes after sunset, a very high rate indeed. In comparison, synthesis of vertebrate photomembrane requires periods of the order of days (Droz, 1967).

The same curves mentioned above point to another aspect of the reassembly process by the coincidence of rapid grain build-up so soon after dusk and that is the link between membrane renewal and a shift in light phase. Although there is disagreement in the literature as to components regulating breakdown and resynthesis of photomembrane (neuroendocrine, local circadian controls, states of illumination), the onset of darkness clearly has a triggering, if not regulatory, effect on resynthesis.

With regard to preceding arguments concerning temporal decay curves, it is interesting to review a few papers in which autoradiography was used to examine light and dark-adapted photomembrane changes. The grain count in honeybee drone visual cells was reported to peak at 48 hours after injection (Pepe and Bauman, 1972), crayfish at 12 hours (Hafner and Bok, 1977), Limulus at 8 hours (Burnel, et al., 1970), and

mosquitoes at 2 hours (Brammer et al., 1978). The time discrepancies may reflect different cellular processes or differences in experimental procedures. More importantly, rigid 12L:12D lighting conditions were not incorporated, a condition known to have abnormal effects on cellular morphology in some species. No information was given in any of the papers concerning the clock time for animal sacrifice. The data on peak concentration time as well as grain path may be in disagreement since experiments were not performed with concern for diurnal cycles. Although it has been shown that recycling of photomembrane is independent of a 24-hour program of sunlight and darkness in the mosquito (White and Lord, 1979), knowledge of diurnal influence on membrane cycling is essential to proper experimental design and interpretation of data.

The Breakdown Phase

Data from retinula cells examined at early morning hours can be interpreted in a couple of ways. First, the presence of silver grains over cytoplasmic areas could mean that protein synthesis continues in the light-adapted state. The likelihood of continued availability of tritiated leucine from the hemolymph supports such an interpretation. However, one cannot rule out the possibility that some of the cytoplasmic label represents protein incorporated into cellular components not directly related to rhabdomere or opsin synthesis.

Another process separate from, but coincident with, protein synthesis can be seen in viewing concurrent events in all three curves

in Figure 5; that is, photomembrane breakdown. While the upper temporal curve maintains a steady count through the three sunrise samples, the lower two curves show a decrease in concentration of counts in the rhabdom to a more equal distribution with the cytoplasm. Although some of the gain in count in the cytoplasm may be due to newly-labeled protein, a more likely interpretation is a loss of protein from the rhabdome to the cytoplasm as photomembrane breakdown products are removed from the rhabdom, possibly for recycling. Implied in this interpretation, though not clearly evident from the data, is initiation of the breakdown process by light.

Long-Term Results

Twenty-four hours after injection, the total grain count in retinula cells had dropped to a level considerably lower than dawn counts. Possibly loss of protein from the rhabdom continued throughout the daylight hours while at some point the cytoplasm began to lose protein from the cell altogether. The continued presence of label in the rhabdom two hours before sunset means either that on a daily basis the rhabdom in Hemigrapsus is not completely degraded as in Leptograpsus or that some breakdown products from the light phase remain in the rhabdom during the next renewal.

Grain concentration for the second day reached a value similar to that for 30 minutes after injection and by seven days was barely detectable. However, distribution continued to favor the rhabdom and since it was unlikely that label was still evolving from newly-synthesized protein, it is possible that some protein was being

recycled.

A curious aspect of all the decay curves is the presence of a decline in grain density several hours after sunset. Since silver grains are assumed to represent only newly-synthesized protein and since renewal and not degradation is known to occur during the dark phase, there should be no decrease. The curves should build to a plateau and maintain until sunrise. Although the curve for Experiment I (Figure 3) shows a plateau at hours 4, 5, and 6 after sunset and the proximity of grain density values for later evening counts to sunrise counts in Experiment II (Figure 5) suggest a plateau, the presence in both experiments of a decrease in grain density preceding plateau formation is contradictory to a synthetic state.

One source of interference may originate from an exchange of free leucine between the hemolymph and retinal tissue. As the initial concentration of H^3 -leucine in the hemolymph is high, some of the grain count in ommatidia may represent unbound leucine undergoing equilibrium diffusion with lymph fluid. That leucine which is not used for protein synthesis may later diffuse from retinal tissue back into the hemolymph as the concentration in the latter compartment decreases (perhaps from uptake by other tissues). It is likely that the true decay curve for newly-synthesized protein is being masked by free leucine diffusing in and out of retinal cells, especially during the early hours after injection. In order to draw a clearer picture of the evolution of new protein, it may be necessary to design a technique to either void the hemolymph of leucine after initial

exposure or to differentiate bound from free leucine.

A final complication in this experiment was a consistently high standard deviation for all grain counts (18-25%), even though all SEM values were within an acceptable 4-5% range. The problem discussed above may have contributed some diffusion. However, since no two rhabdomes or rhabdomeres within the same rhabdom undergo synthesis or breakdown at the same time or rate, it may be difficult to be numerically exact in evaluating membrane cycling. Even experiments using EM Autoradiography, which allows higher resolution, did not produce better statistics (SEM range 4-26% in Perrelet paper, 1972; SEM range 5-22% in Krauhs paper, 1977). However, the broad range in SEM values from these papers was in part due to relatively low ommatidial counts per animal (no reference, Perrelett; average 11 ommatidia per Limulus, Krauhs). Until a more precise technique is developed for assaying protein synthesis in ommatidia, autoradiography (light and EM) is useful only for reflecting general trends in cellular events.

SUMMARY

Autoradiography of tritiated leucine in retinal cells of Hemigrapsus nudus showed differential paths of migration of newly-synthesized protein. Synthesis achieved a maximum rate within an hour after sunset, at which point lateral preference for labeling had switched from the cytoplasm to the rhabdom. Proximal-distal patterns showed a preference for labeled protein in areas peripheral to the microvilli. Morning and long-term samples showed an overall loss in labeled protein while continuing to concentrate protein within the rhabdom.

LITERATURE CITED

- Barlow, R. B., Chamberlain, S. C., Levinson, J. Z. Limulus brain modulates the structure and function of the lateral eyes. *Science* 210, 1037-1039 (1980)
- Basinger, S., Hoffman, R., Mathes, M. Photoreceptor shedding is initiated by light in the frog retina. *Science* 194, 1074-1076 (1976)
- Besharse, Hollyfield, J. G., Rayborn, M. E. Turnover of rod photoreceptor outer segments: I. Membrane addition and loss in relationship to light. *J. Cell Biol.* 75, 490-506 (1977)
- Besharse, Hollyfield, J. G., Rayborn, M. E. Turnover of rod photoreceptor outer segments: II. Membrane addition and loss in relationship to light. *J. Cell Biol.* 507-527 (1977)
- Blest, A. D. The rapid synthesis and destruction of photoreceptor membrane by a dinopid spider: a daily cycle. *Proc. R. Soc. London B.* 200, 463-483 (1978)
- Blest, A. D., Kao, L., Powell, K. Photoreceptor membrane breakdown in the spider Dinopsis: the fate of rhabdomere products. The Effects of Constant Light on Visual Process, Edited by T. P. Williams and B. H. Baker. New York and London: Plenum, pp. 271-296 (1980)
- Blest, A. D., Powell, K., Kao, L. Photoreceptor membrane breakdown in the spider Dinopsis: GERL differentiation in the receptors. *Cell and Tissue Res.* 195, 277-297 (1978)
- Blest, A. D., Maples, J. Exocytotic shedding and glial uptake of photoreceptor membrane by a salticid spider. *Proc. R. Soc. London B.* 204, 105-112 (1979)
- Blest, A. D., Price, G. D., Maples, J. Photoreceptor membrane breakdown in the spider Dinopsis: localization of acid phosphatases. *Cell and Tissue Res.* 199, 455-472 (1979)
- Blest, A. D., Stowe, S., Price, D. G. The sources of acid hydrolyases for photoreceptor membrane degradation in a grapsid crab. *Cell and Tissue Res.* 205, 229-244 (1980)
- Blest, A. D., Williams, D. S. Extracellular shedding of photoreceptor membrane in the open rhabdom of a tipulid fly. *Cell and Tissue Res.* 205, 423-438 (1980)
- Blest, A. D., Williams, D. S., Kao, L. Posterior median eye of Dinopsid spider Menneus. *Cell and Tissue Res.* 211, 391-403 (1980)

- Blest, A. D., deCourt, H. C. The retinal acid phosphatase of a crab *Leptograpsus*: characterization and relation to the cyclical turnover of photoreceptor membrane. *J. Comp. Physiol.* 149, 353-362 (1982)
- Brammer, J. D., Stein, P. J., Andersen, R. A. Effect of light and dark adaptation upon the rhabdom in the compound eye of the mosquito. *J. Exp. Zool.* 206, 151-156 (1978)
- Burnel, M., Mahler, H. R., Moore, W. J. Protein synthesis in visual cells of *Limulus*. *J. Neurochem.* 17, 1493-1499 (1970)
- Chamberlain, S. C., Barlow, R. B. Light and efferent activity control rhabdom turnover in *Limulus* photoreceptor. *Science* 206, 361-363 (1979).
- Droz, B. Dynamic conditions of proteins in the visual cells of rats and mice as shown by radioautography with labeled amino acids. *J. Microscopie* 6, 201 (1967)
- Droz, B. and Warshawsky, H. Reliability of radioautographic technique for the detection of newly synthesized protein. *J. Histochem Cytochem* 11, 426 (1963)
- Eakin, R. M., Brandenburger, J. L. Fine structure of the eyes of jumping spiders. *J. Ultrastructure Res.* 37, 618-663 (1971)
- Eguchi, E. and Waterman, T. H. In, The Functional Organization of the Eye, Edited by C. G. Bernhard. Oxford: Pergamon, pp. 105-124 (1966)
- Eguchi, E., Waterman, T. H., Akiyoma, J. Localization of the violet and yellow receptor cells in the crayfish retinula. *J. General Physiol.* 62, 355-374 (1973)
- Eguchi, E., Waterman, T. H. Freeze-etch and histochemical evidence for cycling in crayfish photoreceptor membranes. *Cell and Tissue Res.* 169, 419-434 (1976)
- Frixione, E. and Arechiga, H. Photomechanical migration of pigment granules along the retinal cells of the crayfish. *J. Neurobiol.* 10:573-590 (1979)
- Hafner, G. S., Bok, D. Distribution of ³H-leucine labeled protein in the retinula cells of the crayfish retina. *J. Comp. Neuro.* 174, 397-416 (1977)
- Hafner, G. S., Hammond-Soltis, G., Tokarski, T. Diurnal changes of lysosome-related bodies in the crayfish photoreceptor cells. *Cell and Tissue Res.* 206, 319-322 (1980)

- Hall, M. O., Box, D., Bacharach, A. D. E. Biosynthesis and assembly of the rod outer segment membrane system. Formation and fate of visual pigment in the frog retina. *J. Mol. Biol.* 45, 397-406 (1969)
- Hollyfield, J. C., Besharse, Rayborn, M. E. Photoreceptor outer segments: accelerated membrane renewal in rods after exposure to light. *Science* (Washington, D. C.) 196, 536-538 (1977)
- Horridge, G. A. and Barnard, P. B. T. Movement of palisade in locust retinula cells when illuminated. *Quart. J. Micro. Sci.* 106, 131-135 (1965)
- Horridge, G. A. and Blest, D. The Compound Eye. In, Insect Biology of the Future, by Michael Locke and D. S. Smith. New York: Academic Press (1980)
- Itaya, S. K. Rhabdom changes in the shrimp, *Palaemonetes*. *Cell and Tiss. Res.* 169, 419-434 (1976)
- Kraus, J. M., Mahler, H. R., Moore, W. J. Protein turnover in photoreceptor cells of the isolated *Limulus* lateral eyes. *J. of Neurochem.* 30, 625-632 (1978)
- Langer Helmut (Editor). Biochemistry and Physiology of Visual Pigments. New York, Heidelberg, and Berlin: Springer-Verlag (1973)
- LaVail, M. M. Rod outer segment disc shedding in relation to cyclic lighting. *Exp. Eye Res.* 23, 277-280 (1976)
- LaVail, M. M. Rod outer segment disc shedding in rat retina: relationship to cyclic lighting. *Science* (Washington) 194, 1071-1074 (1976)
- Nassel, D. R., Waterman, T. H. Massive diurnally modulated photoreceptor membrane turnover in crab light and dark adaptation. *J. Comp. Physiol.* 131, 205-216 (1979)
- O'Day, W. T., Young, R. W. Rhythmic daily shedding of outer segment membrane by visual cells in goldfish. *J. Cell Biol.* 76, 593-604 (1978)
- Ottoson, D. Physiology of the Nervous System. New York: Oxford University Press (1983)
- Pepe, I. M., Bauman, F. Incorporation of ^3H -labeled leucine into the protein fraction of the retina of the honeybee drone. *J. of Neurochem.* 19, 507-512 (1972)
- Perrelet, Alain. Protein synthesis in the visual cells of the honeybee drone as studied with EM autoradiography. *J. of Cell Biol.* 55, 595-605 (1972)

- Peters, T., Jr. and Ashley, C. A. An artifact in radioautography due to binding of free amino acids to tissues by fixative. *J. Cell. Biol.* 33, 53-60 (1967)
- Pietzsch-Rohrschneider. Scanning EM of photoreceptor cells in the light and dark-adapted retina of Haplochromis burtoni (Cichlidae, Teleostei). *Cell and Tiss. Res.* 175, 123-130 (1976)
- Prince, J. H. Comparative Anatomy of the Eye. Springfield, Illinois: C. Thomas (1956)
- Shepherd, G. M. Neurobiology. New York: Oxford University Press (1983)
- Stowe, S. Rapid synthesis of photoreceptor membrane and assembly of new microvilli in a crab at dusk. *Cell and Tiss. Res.* 211: 419-440 (1980)
- Stowe, S. Effects of illumination changes on rhabdom synthesis in the crab. *J. Comp. Physiol.* 1-2, 19-25 (1981)
- Stowe, S. Rhabdom synthesis in isolated eyestalks and retinæ of the crab *Leptograpsus variegatus*. *J. Comp. Physiol.* 158, 313-321 (1982)
- Waterman, T. H. Expectation and achievement in comparative physiology. *J. Exp. Zool.* 194, 309-343 (1975)
- Waterman, T. H., Eguchi, E. Fine structure patterns in crustacean rhabdomes. In, The Functional Organization of the Compound Eye, Edited by C. G. Bernhard. New York: Pergamon Press (1966)
- Waterman, T. H., Horch, K. W. Mechanism of polarized light perception. *Science* 154, 467-475 (1966)
- White, R. H. Effect of light and light deprivation upon the ultrastructure of the larval mosquito eye. *J. Exp. Zool.* 166, 405-426 (1967)
- White, R. H. Effect of light and light deprivation upon the ultrastructure of the larval mosquito eye. III. Multivesicular bodies and protein uptake. *J. Exp. Zool.* 169, 261-278 (1968)
- White, R. H., Lord, E. Diminution and enlargement of the mosquito rhabdom in light and darkness. *J. General Physiol.* 65, 583-598 (1975)
- White, R. H., Sundeen, C. D. The effect of light and light deprivation upon the ultrastructure of larval mosquito eye. *J. Exp. Zool.* 164, 461-478 (1967)

White, R. H., Gifford, D. Michaud, N. Turnover of photomembrane in the larval mosquito Ocellus: rhabdomeric coated vesicles and organelles of the vacuolar system. In, The Effects of Constant Light on the Visual Process, Edited by T. P. Williams and B. N. Baker. New York: Plenum Press, pp. 271-296 (1980)

Williams, David S. Rhabdom size and photoreceptor membrane turnover in a muscoid fly. *Cell Tiss. Res.* 226, 629-639 (1982)

Young, R. W. The renewal of photoreceptor cell outer segments. *J. of Cell Biol.* 33, 61-72 (1967)

Young, R. W., Droz, B. The renewal of protein in retinal rods and cones. *J. of Cell Biol.* 39, 169-184 (1968)